

## Electrical property measurements of Cr-N codoped TiO<sub>2</sub> epitaxial thin films grown by pulsed laser deposition

J. Jaćimović, R. Gaál, A. Magrez, L. Forró, M. Regmi et al.

Citation: *Appl. Phys. Lett.* **102**, 172108 (2013); doi: 10.1063/1.4804240

View online: <http://dx.doi.org/10.1063/1.4804240>

View Table of Contents: <http://apl.aip.org/resource/1/APPLAB/v102/i17>

Published by the [American Institute of Physics](#).

---

### Additional information on *Appl. Phys. Lett.*

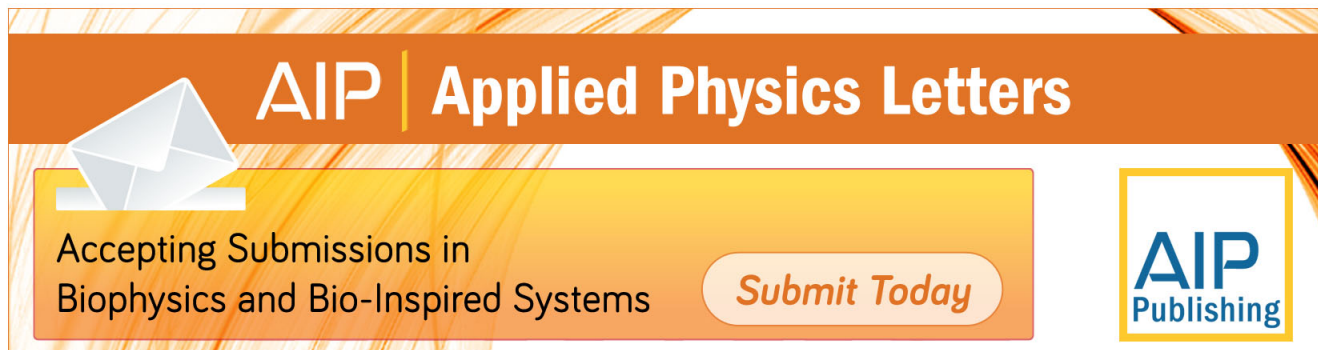
Journal Homepage: <http://apl.aip.org/>

Journal Information: [http://apl.aip.org/about/about\\_the\\_journal](http://apl.aip.org/about/about_the_journal)

Top downloads: [http://apl.aip.org/features/most\\_downloaded](http://apl.aip.org/features/most_downloaded)

Information for Authors: <http://apl.aip.org/authors>

## ADVERTISEMENT



**AIP** | Applied Physics Letters

Accepting Submissions in  
Biophysics and Bio-Inspired Systems

*Submit Today*

**AIP**  
Publishing

## Electrical property measurements of Cr-N codoped TiO<sub>2</sub> epitaxial thin films grown by pulsed laser deposition

J. Jaćimović,<sup>1</sup> R. Gaál,<sup>1</sup> A. Magrez,<sup>1</sup> L. Forró,<sup>1</sup> M. Regmi,<sup>2</sup> and Gyula Eres<sup>2</sup>

<sup>1</sup>Ecole Polytechnique Fédérale de Lausanne, Laboratory of Physics of Complex Matter, CH-1015 Lausanne, Switzerland

<sup>2</sup>Materials Science and Technology Division, Oak Ridge National Laboratory, Oak Ridge, Tennessee 37831, USA

(Received 26 February 2013; accepted 19 April 2013; published online 3 May 2013)

The temperature dependent resistivity and thermo-electric power of Cr-N codoped TiO<sub>2</sub> were compared with that of single element N and Cr doped and undoped TiO<sub>2</sub> using epitaxial anatase thin films grown by pulsed laser deposition on (100) LaAlO<sub>3</sub> substrates. The resistivity plots and especially the thermoelectric power data confirm that codoping is not a simple sum of single element doping. However, the negative sign of the Seebeck coefficient indicates electron dominated transport independent of doping. The narrowing distinction among the effects of different doping methods combined with increasing resistivity of the films with improving crystalline quality of TiO<sub>2</sub> suggest that structural defects play a critical role in the doping process.

© 2013 AIP Publishing LLC. [<http://dx.doi.org/10.1063/1.4804240>]

In addition to inducing conductivity, doping is a widely studied approach for narrowing the band gap in oxide semiconductors. Bandgap narrowing is the main avenue for shifting the absorption band of titanium dioxide (TiO<sub>2</sub>) into the visible spectral region that is needed for improving the currently low conversion efficiency of solar into other forms of energy using photocatalytic processes. Doping of TiO<sub>2</sub> is typically performed by substitution of either Ti atoms known as cation doping, or O atoms known as anion doping.<sup>1,2</sup> There is extensive literature addressing various aspects of doping using density functional theory (DFT) and other methods, which show that the electronic states created by cation and anion doping reside in distinctly different regions of the electronic band structure of TiO<sub>2</sub>.<sup>3,4</sup> However, experimental studies of doping in TiO<sub>2</sub> find that single element doping using either cations or anions often has only a weak effect on the bandgap, or it creates localized states in the bandgap that hinder efficient charge transport.<sup>5</sup>

Single element doping is also subject to thermodynamic and kinetic solubility barriers that if sufficiently large prevent reaching doping concentrations necessary for producing effective bandgap narrowing. To overcome the shortcomings of single element doping, a doping scheme that involves simultaneous incorporation of a cation-anion pair referred to as codoping is being explored. Codoping comes in two flavors. If the oxidation states of the two dopants are equal, codoping is compensated,<sup>6</sup> and if the oxidation states are not balanced, non-compensated codoping results.<sup>7</sup> DFT calculations by Zhu *et al.* show that only non-compensated codoping creates electronic states that contribute to significant bandgap narrowing.<sup>7</sup> Accordingly, DFT calculations using N(+1) and Cr(-2) as a non-compensated pair predict a bandgap near 1.5 eV in anatase TiO<sub>2</sub>, that was confirmed using scanning tunneling spectroscopy in 1%–2% Cr-N codoped anatase nanoclusters synthesized by sol-gel methods.<sup>7</sup>

An important factor that affects all doping methods is related to the ability of TiO<sub>2</sub> to exist in highly nonstoichiometric forms.<sup>8</sup> This nonstoichiometry causes unintentional

doping often referred to as self-doping characterized by electronic states generated by vacancies, including both under-coordinated Ti and O atoms, and structural defects in TiO<sub>2</sub>.<sup>9</sup> In highly defective material, self-doping can produce large variations in conductivity and obscure or even dominate intentional doping. Forró and co-workers<sup>10</sup> reported that the resistivity of single crystal anatase with oxygen deficiency can vary between 10<sup>-1</sup> and 10<sup>1</sup> Ωcm, and exhibits metal-like characteristics ( $d\rho/dT > 0$ ) in the 300–60 K temperature range. It was suggested that this conductivity occurs because of the formation of shallow impurity levels near the conduction band minimum (CBM). The width of the impurity band was found to depend on the concentration of oxygen vacancies, changing the absolute value of the resistivity accordingly.<sup>11</sup> Additional information obtained from high pressure transport studies reveals that conductivity in TiO<sub>2-x</sub> single crystals occurs by polaron transport.<sup>11</sup>

Although TiO<sub>2</sub> doping is widely studied and a large number of theoretical and experimental papers have been published on various aspects of doping, there are few reports that address electrical properties.<sup>12,13</sup> This is mainly because the resistivity of TiO<sub>2</sub> is too high for routine measurement at or below room temperature. Another notable factor is that most of currently grown doped anatase is of poor crystalline quality, which obscures the interpretation of the measurements. For example, the nanoclusters produced by sol-gel synthesis—the method favored for exploration of TiO<sub>2</sub> doping—typically contain a range of compositions, including different phases and amorphous inclusions making it difficult to identify unambiguously doping related effects. In this letter, we use electrical resistivity and thermo-electric power (TEP) measurements of anatase thin films to compare the effectiveness of the non-compensated codoping method with conventional single element doping in changing the intrinsic properties of anatase TiO<sub>2</sub>. Specifically, the temperature dependent electrical property measurements are used to gain insight into the type and the location of the electronic states created by a specific dopant or doping method.

The thin films of undoped, Cr only, N only doped, and Cr-N codoped anatase of 40 nm typical thickness were grown on LaAlO<sub>3</sub> (100) substrates at a fixed temperature of 780 K. The undoped films were grown from a pure TiO<sub>2</sub> target. Cr only doped anatase films were prepared from a Cr containing TiO<sub>2</sub> target, while N doping was performed from N<sub>2</sub> in the background gas of the pulsed laser deposition (PLD) chamber. The Cr-N codoped anatase films were prepared by using N containing compounds of either Cr or Ti in the PLD target. In addition, the N content of Cr-N films was supplemented by simultaneous doping from the gas phase background. For all samples, the background pressure was fixed using a total gas flow of 6 sccm. However, the composition of the background gas was changed to control both the oxidative environment and the N doping level of the anatase films. The fully oxidized TiO<sub>2</sub> samples were grown at a total pressure of  $1.5 \times 10^{-5}$  mbar composed of N<sub>2</sub> and O<sub>2</sub> in 5:1 ratio for N doping. In undoped and samples without N doping, N<sub>2</sub> was replaced by Ar to maintain a fixed total pressure. The presence of dopants in the films was confirmed by XPS. N doped films contained not just the interstitial (weakly bound molecular) N around 400 eV binding energy (BE), but the substitutional (nitridic) N at 396 eV BE. The dopant concentrations were around 0.5% for N, 1% for Cr, and above 1% for Cr-N. The observation of a weak low BE shoulder on the Ti 2p peak in undoped and N doped films is indicative of a reduced surface. The resistivity measurements in the 4 to 900 K range were performed by a standard four point technique. The electrical leads were gold wires attached to pre-evaporated gold pads using silver paste to ensure stable electrical contacts. The thermo-electric power measurements were performed by using a small heater attached to one end of the substrate to generate a temperature gradient that was measured by a chromel-constantan differential thermocouple.<sup>14</sup>

The temperature dependent resistivity of fully oxidized TiO<sub>2</sub> films is difficult to measure because the room temperature values even for doped films are in the MΩ range. To produce conductive samples, we intentionally introduce oxygen vacancies by reducing the oxygen pressure during film growth about an order of magnitude while keeping all other parameters unchanged. The conductivity of these samples is attributed to extra electrons that become available by the formation of oxygen vacancies. The films grown under oxygen poor conditions were also useful for estimating the extent and the effects of self doping on TiO<sub>2</sub>. The partial pressure of oxygen was still sufficient to produce crystalline anatase films. However, x-ray diffraction (XRD) rocking curves of the (004) anatase peak show that these films have a mosaic spread in the range from 0.15° to 0.3° FWHM, which is roughly 3 times larger than that for fully oxidized films, suggesting a lower degree of structural perfection attributed to grain boundaries and other defects where oxygen vacancies can segregate and accumulate. The anatase (004) FWHM values for the fully oxidized films are comparable to the best crystalline quality Cr doped anatase films grown by MBE at low growth rate reported by Kaspar.<sup>15</sup> The most important difference between the two groups is that the films in the optimally oxidized group have a much higher resistivity than the respective films produced under oxygen deficient conditions, consequently, the films in the

two sets are also referred to as high and low resistivity samples, respectively.

The temperature dependent resistivity plots illustrated in Fig. 1 show that despite the nominally same dopant composition during growth the samples fall into two distinct groups. The films grown at optimal oxygen pressure have a high room temperature resistance and were measurable only at high temperatures, while the films grown at oxygen deficient conditions were conductive at room temperature and could be measured down to low temperatures. The high resistivity films show a history (illustrated for the undoped and Cr-N doped films in Fig. 1) with thermal cycling. During the warming cycle, the resistivity is much higher than at the same temperature of the cooling cycle. This behavior is ascribed to oxygen loss and the formation of vacancies, the configuration and concentration of which stabilizes at lower temperatures.

The resistivity curves in Fig. 1 are described by the following activated behavior:

$$\rho = \rho_0 \exp(E_d/k_B T), \quad (1)$$

where  $E_d$  is the activation energy,  $\rho_0 \sim (\mu n_0)^{-1}$  contains the non-activated part of the resistivity (the mobility and the total carrier density) and  $k_B$  is the Boltzmann constant. The fitted values of  $E_d$  shown in Fig. 2 are for all samples lower than the intrinsic band gap of anatase. The activation energy for the low resistivity anatase films is about two orders of magnitude lower as shown in Fig. 2. The resistivity of oxygen deficient films gradually increases with the activation energy approaching 1 eV (data not shown) when exposed to oxygen atmosphere at 700 K. This trend is a strong indication that the higher conductivity of these films is related to oxygen vacancy related carriers. The resistivity of N doped samples appears even metal-like in a broad temperature range. Only below 100 K, it shows a semiconducting behavior with  $E_d$  of

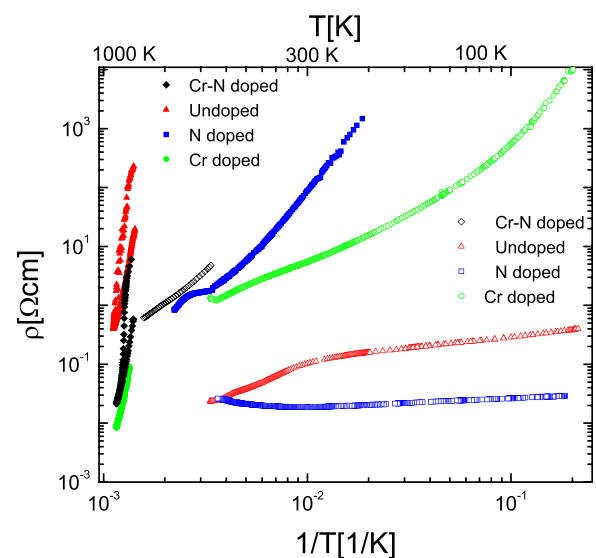


FIG. 1. The temperature dependent resistivity data for the two sets of anatase thin films. The films grown in low oxygen environment are designated by open symbols and the optimally oxidized films are represented by solid color symbols. The type of doping is described by black diamonds for Cr-N codoped, red triangles for undoped, green circles for Cr, and blue squares for N only doped anatase.

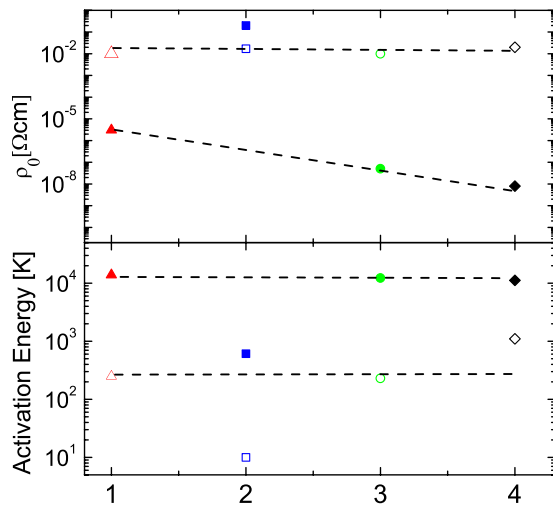


FIG. 2. The activation energy of the impurity levels and the resistivity prefactors  $\rho_0$  deduced from Fig. 1 for the high (solid symbols) and low (open symbols) resistivity films for 1 undoped, 2 N only doped, 3 Cr only doped, and 4 Cr-N codoped anatase films.

10K. Despite their lower resistivity, the prefactors  $\rho_0$  shown in Fig. 2 are much higher for the low resistivity films than for the high resistivity films. Since the carrier density is likely to be higher in these samples because of the increased oxygen vacancy concentration, the origin of the increased prefactor is in the deterioration of the mobility. It is difficult to reconcile the large difference in the activation energies for high and low resistivity anatase thin films within the simple doped semiconductor picture where the impurity level is proportional to  $m^*/\epsilon^2$ , the effective mass and the dielectric constant. Neither of these quantities depends on the density of dopants. A possible explanation for this behavior is that at low dopant concentration charge transport occurs by thermal excitation from the impurity level into the CBM, while at high doping level it proceeds by hopping conduction within the impurity band. Polaron hopping is the accepted mechanism for electron transport in bulk  $\text{TiO}_2$ .<sup>16</sup> With the combination of increasing disorder and the presence of localized states created by doping, the variable range hopping (VRH) model becomes a viable description.<sup>17</sup> The VRH model was recently found by Zhao *et al.*<sup>18</sup> to provide a good description for the conductivity of PLD grown  $\text{TiO}_2$  films at variable oxygen pressure. In contrast, the conductivity in 5 of our anatase films occurs at higher temperatures than that reported above, and none of the remaining 3 films with low temperature conductivity exhibit VRH type behavior. It is well-known that the VRH in Mott's description is a single phonon assisted process effective at low temperatures. At higher temperatures, multi-phonon processes dominate and introduce further temperature dependence, which causes a deviation from the canonical, single exponent description of VRH. A further source for the discrepancy of the resistivity data with a single exponent is the microstructure of the grain boundaries, which introduce an additional barrier in the hopping term.<sup>19</sup> Similarly, grain boundary oxygen vacancy interactions were found instrumental for the ferromagnetic behavior of Co and Cr doped anatase nanocrystals.<sup>20</sup> We attribute the lack of agreement with the VRH model to the high crystalline quality and possibly to the low dopant concentrations in our anatase films.

The type of the charge carriers is given by the sign of the Seebeck coefficient  $S$  determined by the TEP measurement. The TEP for the low resistivity undoped, Cr only, N only doped, and Cr-N doped anatase samples is illustrated in Fig. 3. The large noise caused by the high resistance prevented reliable TEP measurements of the high resistivity films. Electron dominated transport corresponds to a negative  $S$ , while for hole transport  $S$  has a positive sign. The data in Fig. 3 show that  $S$  is negative even for the N doped sample, which is expected to be hole doped. Note the distinctly different behavior of the Cr-N codoped films in Fig. 3. We use simple charge counting to discuss the possible outcomes of doping. If Cr doping transfers 6 electrons and replaces  $\text{Ti}^{4+}$ , the net gain is 2 electrons. N doping transfers 3 holes and replaces oxygen introducing net 1 hole per formula unit. However, XPS spectra show  $\text{Cr}^{3+}$  in anatase.<sup>15,21</sup> If such Cr replaces Ti, it introduces an extra electron per formula unit. In the case of codoping, the charge counting is more complex, since the Cr to N ratio was found to deviate from a 1:1 ratio. The fact that the Seebeck coefficient is negative in all cases suggests that electrons introduced by oxygen vacancies dominate the charge transport in all anatase thin films according to the relationship  $\text{Ti}_{1-x}^{4+}\text{Ti}_x^{3+}(\text{O}_{2-x}^{2-}) + xe^-$ .

The temperature dependence of TEP of a semiconductor is expected to vary as  $k_B/q(E_d/k_B T)$ , where  $q$  is the electronic charge. None of the curves in Fig. 3 follows such dependence. Rather they show near linear temperature variation similar to metals but the high value and the temperature dependence of the resistivity are incompatible with a metallic conduction mechanism. It is instead compatible with the hopping nature of charge transport. In this case,  $dS/dT$  is positive<sup>22</sup> but  $S$  is usually only a few  $\mu\text{V/K}$ . The fact that in our  $\text{TiO}_2$  samples  $S$  is in the 100 s  $\mu\text{V/K}$  range could come from the polaronic character of the charge carriers in anatase similar to TEP in pristine single crystals that was demonstrated in a recent study.<sup>23</sup> According to this interpretation, because of strong electron phonon coupling, the charge carrier polarizes the lattice and a quasiparticle, the polaron forms. The temperature dependence is governed by the microscopic parameters of the polaron formation and transport.

In summary, temperature dependent TEP measurements show that the behavior of Cr-N codoped anatase films is markedly different from single element Cr, and N doped anatase films. The temperature dependent resistivity data show

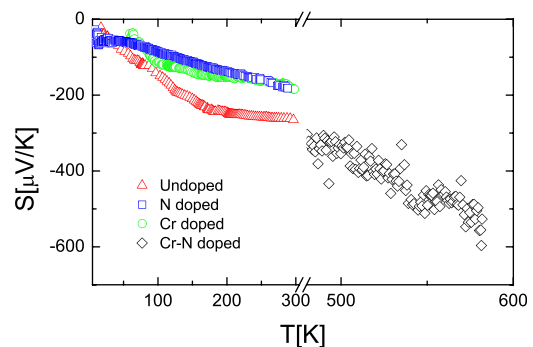


FIG. 3. Thermo-electric power as a function of temperature for the low resistivity samples. Note that the sign of the TEP is negative even for N doped anatase.

that this distinction narrows with improving crystalline quality of the anatase films that are grown at optimal oxidation conditions during growth. All samples show activated conductivity, but the activation energy is  $\sim 1$  eV for samples grown in optimal oxygen atmosphere while it is  $\sim 0.1$  eV for samples grown under oxygen deficient conditions. The negative Seebeck coefficient indicates electron conductivity for all films independent of the dopant type. The TEP of all samples shows high absolute value but atypical temperature dependence for a semiconductor. This fact, together with the low mobility of the samples points toward hopping conduction of polarons in doped anatase. The main conclusion of this work is that independent of the doping method and the dopant type, the data show that structural defects facilitate dopant incorporation. Similarly, the interplay between structural defects and oxygen vacancies was found instrumental for manifestation of ferromagnetism in Co and Cr doped anatase nanocrystals and MBE grown anatase films.<sup>15,20</sup> Experiments addressing whether favorable defects must be present already for doping to occur, or doping itself is accompanied by simultaneous creation of certain structural defects are currently underway.

The work in Lausanne was supported by the Swiss NSF through its research network “MaNEP.” The work at Oak Ridge National Laboratory was supported by the U.S. Department of Energy, Basic Energy Sciences, Materials Sciences and Engineering Division. The authors thank Endre Horváth for fruitful discussions.

<sup>1</sup>W. Choi, A. Termin, and M. Hoffmann, *J. Phys. Chem.* **98**, 13669 (1994).

<sup>2</sup>R. Asahi, T. Morikawa, T. Ohwaki, K. Aoki, and Y. Taga, *Science* **293**, 269 (2001).

<sup>3</sup>H. Wang and J. Lewis, *J. Phys.-Condens. Matter* **18**, 421 (2006).

- <sup>4</sup>T. Umebayashi, T. Yamaki, H. Itoh, and K. Asai, *J. Phys. Chem. Solids* **63**, 1909 (2002).
- <sup>5</sup>T. L. Thompson and J. T. Yates, Jr., *Chem. Rev.* **106**, 4428 (2006).
- <sup>6</sup>Y. Gai, J. Li, S.-S. Li, J.-B. Xia, and S.-H. Wei, *Phys. Rev. Lett.* **102**, 036402 (2009).
- <sup>7</sup>W. Zhu, X. Qiu, V. Iancu, X.-Q. Chen, H. Pan, W. Wang, N. M. Dimitrijevic, T. Rajh, H. M. Meyer, M. P. Paranthaman, G. M. Stocks, H. H. Weitering, B. Gu, G. Eres, and Z. Zhang, *Phys. Rev. Lett.* **103**, 226401 (2009).
- <sup>8</sup>Q. He, Q. Hao, G. Chen, B. Poudel, X. Wang, D. Wang, and Z. Ren, *Appl. Phys. Lett.* **91**, 052505 (2007).
- <sup>9</sup>J. Nowotny, M. Radecka, and M. Rekas, *J. Phys. Chem. Solids* **58**, 927 (1997).
- <sup>10</sup>L. Forró, O. Chauvet, D. Emin, L. Zuppiroli, H. Berger, and F. Levy, *J. Appl. Phys.* **75**, 633 (1994).
- <sup>11</sup>J. Jaćimović, C. Vaju, R. Gaál, A. Magrez, H. Berger, and L. Forró, *Materials* **3**, 1509 (2010).
- <sup>12</sup>Y. Furubayashi, T. Hitosugi, Y. Yamamoto, K. Inaba, G. Kinoda, Y. Hirose, T. Shimada, and T. Hasegawa, *Appl. Phys. Lett.* **86**, 252101 (2005).
- <sup>13</sup>M. Katayama, S. Ikesaka, J. Kuwano, H. Koinuma, and Y. Matsumoto, *Appl. Phys. Lett.* **92**, 132107 (2008).
- <sup>14</sup>J. Jacimovic, R. Gaal, A. Magrez, J. Piatek, L. Forro, S. Nakao, Y. Hirose, and T. Hasegawa, *Appl. Phys. Lett.* **102**, 013901 (2013).
- <sup>15</sup>T. C. Kaspar, S. M. Heald, C. M. Wang, J. D. Bryan, T. Droubay, V. Shutthanandan, S. Thevuthasan, D. E. McCready, A. J. Kellock, D. R. Gamelin, and S. A. Chambers, *Phys. Rev. Lett.* **95**, 217203 (2005).
- <sup>16</sup>N. A. Deskins and M. Dupuis, *Phys. Rev. B* **75**, 195212 (2007).
- <sup>17</sup>S. J. Konezny, C. Richter, R. C. Snoeberger, III, A. R. Parent, G. W. Brudvig, C. A. Schmuttenmaer, and V. S. Batista, *J. Phys. Chem. Lett.* **2**, 1931 (2011).
- <sup>18</sup>Y. L. Zhao, W. M. Lv, Z. Q. Liu, S. W. Zeng, M. Motapothula, S. Dhar, Ariando, Q. Wang, and T. Venkatesan, *AIP Adv.* **2**, 012129 (2012).
- <sup>19</sup>L. Zuppiroli and L. Forro, *Phys. Lett. A* **141**, 181 (1989).
- <sup>20</sup>J. Bryan, S. Santangelo, S. Keveren, and D. Gamelin, *J. Am. Chem. Soc.* **127**, 15568 (2005).
- <sup>21</sup>N. Mannella, C. Cheney, P. Vilmercati, M. Regmi, H. Weitering, and G. Eres, “The physics of noncompensated codoping as a route to band gap narrowing in oxide materials: electronic structure and ultra-fast charge transfer dynamics in Cr/N codoped TiO<sub>2</sub> unveiled with soft-x-ray spectroscopies” (unpublished).
- <sup>22</sup>V. H. Crespi, L. L. Y. X. Jia, K. Khazeni, A. Zettl, and M. L. Cohen, *Phys. Rev. B* **53**, 14303 (1996).
- <sup>23</sup>J. Jacimovic, C. Vaju, A. Magrez, H. Berger, L. Forro, R. Gaal, V. Cerovski, and R. Zikic, *EPL* **99**, 57005 (2012).